An Eco-friendly Porous Poly(imide-ether)s for the Efficient Removal of Methylene Blue: Adsorption Kinetics, Isotherm, Thermodynamics and Reuse Performances

Arukkani Murugesan, M. Divakaran, Pranav Raveendran, A. B. Nitin Nikamanth & Kevin J. Thelly

Journal of Polymers and the Environment
formerly: `Journal of Environmental Polymer Degradation'

ISSN 1566-2543

J Polym Environ
DOI 10.1007/s10924-019-01408-z

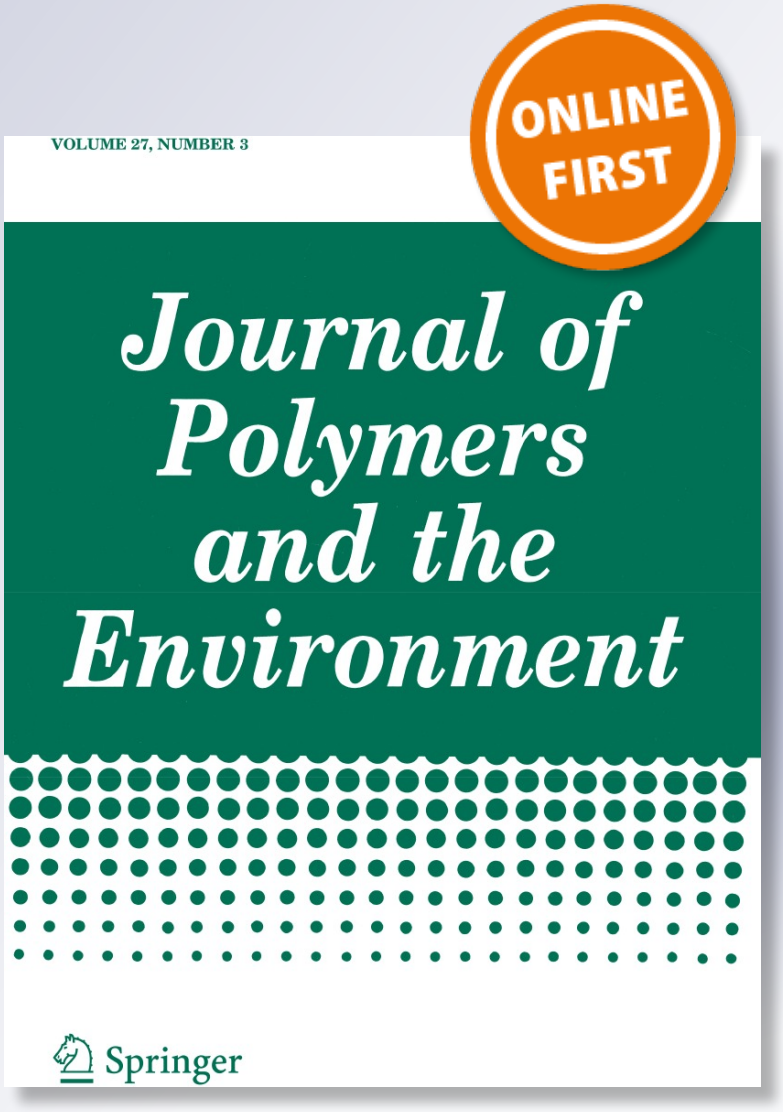

Springer

Journal of Polymers and the Environment
https://doi.org/10.1007/s10924-019-01408-z

ORIGINAL PAPER

An Eco-friendly Porous Poly(imide-ether)s for the Efficient Removal of Methylene Blue: Adsorption Kinetics, Isotherm, Thermodynamics and Reuse Performances

Arukkani Murugesan[1] · M. Divakaran[1] · Pranav Raveendran[2] · A. B. Nitin Nikamanth[2] · Kevin J. Thelly[2]

Abstract

Poly(imide-ether)s (PIEs), which is porous in nature, was synthesized using aromatic diamines and dianhydrides via the solution polycondenzation reaction. In the process, PIEs was used as an adsorbent for the removal of basic dye [Methylene blue (MB)] from the aqueous solution. The structure and the thermal stability of PIEs were characterized by FT-IR, ^{1}H-NMR, XRD and TG analysis, and the adsorption behaviour of the PIEs was confirmed using UV/Visible, FT-IR and SEM with EDX analysis. Batch adsorption experiments were carried out and their parameters (pH 6.95), initial MB concentration (200 mg/L), adsorbent dosage (50 mg), contact time (120 min) and temperature (28 °C) were optimized. The batch adsorption experimental data of the effect of contact time, initial MB concentration and temperature were evaluated using the adsorption kinetics (Pseudo-first order, Pseudo-second order, Elovich and Intra-particle diffusion kinetic), isotherm (Langmuir, Freundlich, Redlich–Peterson and Sips isotherms) and thermodynamic models respectively. In the study, adsorption of MB onto PIEs followed Pseudo-second kinetics and found to be the best fitting model based on the obtained experimental data. The homogeneity and heterogeneity surface nature of PIEs were elucidated with two and three isotherm parameters respectively. The adsorption thermodynamic study indicates that the adsorption of MB onto PIEs was endothermic and spontaneous in nature. The adsorbed PIEs solid waste was utilized to prepare the polymer composite, and its property was characterized.

✉ Arukkani Murugesan
murugesana@ssn.edu.in

[1] Department of Chemistry, SSN College of Engineering, Chennai 603 110, India

[2] Department of Computer Science and Engineering, SSN College of Engineering, Chennai 603 110, India

Published online: 25 February 2019

Graphical Abstract

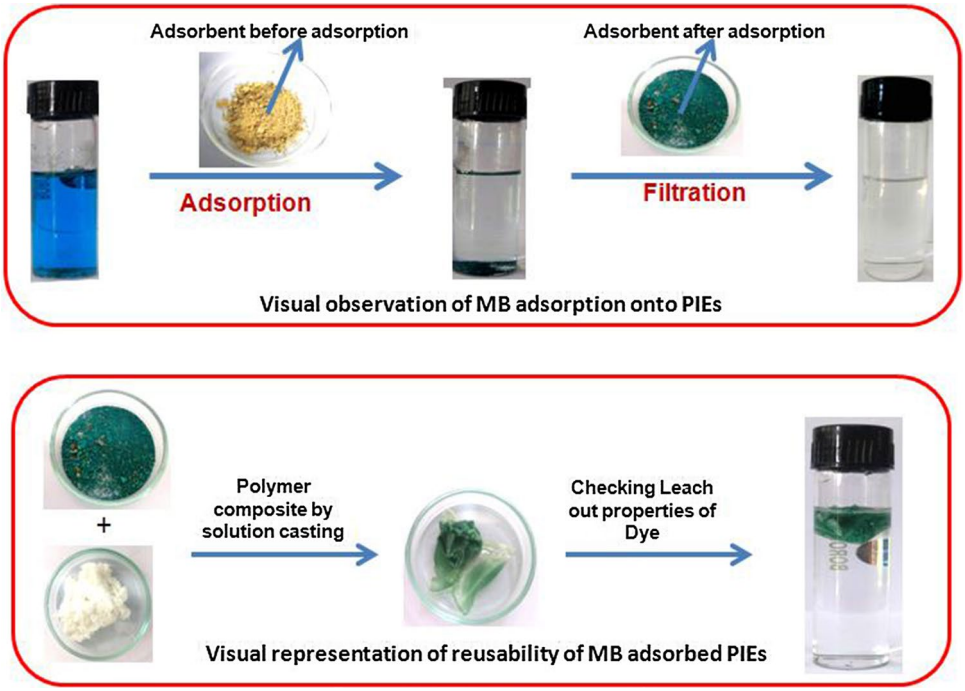

Keywords Poly(imide-ether)s · Methylene blue · Adsorption · Isotherm · Endothermic

Introduction

Organic and inorganic contaminations in the wastewater from textiles, pharmaceutical, metal, refinery and biochemical industries are serious issues in the earthly and aquatic biological communities. Improper disposal of dyes and heavy metal ions into the fresh water causes severe damages in the living and non-living bodies of nature. These pollutants are non-biodegradable and accumulated in the living organism such as animals, plants and human beings.

Wastewater from textile industries also leads uncompromising environmental impact [1]. Textile industries and solar cell industries use various types of organic dyes such as disperse dyes, reactive dyes, mordant dyes, metal-related dyes, anionic (acid) and cationic (basic) dyes for different purposes [2]. A dye discharged without proper purification into the water system causes health risks to living beings, microorganisms and affects the ecosystem. Dyes (colorant) and the auxiliary chemicals of dyes in contact with the skin create allergic reactions (itching, irritations and dermatitis), respiratory issues and also numerous health defects; particularly, MB dye intake leads to mental disorder, fever, nausea and many other diseases which cannot be treated [3–5]. The small amount (< 1 mg/L) of dye present in the water is highly noticeable and toxic, which incredibly spoils the quality of the water system. So, the expulsion of colorant from wastewater is necessary than the evacuation of the dissolvable organic substances.

MB (Scheme 1) is one of the complex basic dyes called as methylthioninium chloride; hydrate state because of hygroscopic in nature which is used for biological purpose to find the structure of cells, tissues and industries for high scale dying of nylon, cotton and other wearable materials. MB is a salt of organic base that dissolves in water as cations which are also called as cationic dye. It is nonbiodegradable and has microbial properties.

Many methods have been established for the removal of pollutants from the aquatic system, such as precipitation, filtration, coagulation, membrane separation, chemical degradation and adsorption process. Among this technical method, adsorption is the most effective, economical,

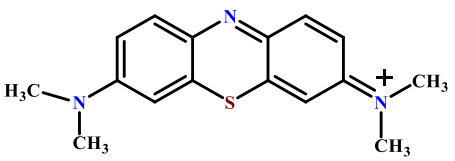

Scheme 1 Chemical structure of Methylene blue (MB)

recyclable, reliable method for the removal of the dyes from the wastewater [6–9]. Past two decades, many adsorbents such as commercial activated carbon (AC) (lignite coal [10]), AC from agricultural wastes (palm kernel shell [11, 12], finger citron [13], coirpith [14], wood apple rind [15], saw dust [16], orange peel [17], corncob [18], apple pomace and wheat straw [19], coconut tree flower and jute fibre carbon [20], rice husk ash [21]) and zeolites have been incorporated for the removal of heavy metal inos and dyes from the industrial effluents [22–24]. AC has a limited surface area and lower regeneration capability which cannot be an efficient adsorbent. To enhance the adsorption capacity, new nano and nano composite materials (magnetite/pectin and magnetitie/silica/pectin hybrid nanocomposites [25], alumina nanoparticles [26], nano-silica fabricated silver nano particles [27], graphene oxide sheet integrated with gold nanoparticles [28], cobalt ferrite nanoparticles [29], nano-sized TiO_2 [30], amino modified SiO_2–Fe_3O_4 nano material [31], reduced graphene oxide [32]) have been developed in the adsorption process. Although nanomaterials are broadly known as an adsorbent, it is still indistinct of what perils certain material can bring to the environment due to its stability, agglomeration (cluster formation leads to a low surface area) and degradation [33].

Recently, high-performance aromatic polymers (HPAPs) have received more interest as a more stable adsorbent for the removal of various water pollutants from industrial wastewater such as heavy metal ions and dyes [34–41]. Porosity, high surface area and highly accessible networking sites bind the water pollutants by intramolecular interaction, electrostatic forces and conjugation effect. It can be enriched on the surface of HPAPs which have been enhanced with the adsorption capacity. The incorporation of donor–acceptor moieties in the polymer back-bone have influenced and made the chemical bonding (donor–acceptor) between polymeric adsorbent and the adsorbate (metal ions and dyes) [42–44].

This work focuses on synthesizing porous poly(imide-ether)s (PIEs) adsorbent materials with imide-ether functional moieties via polycondensation technique, and its application for the removal of MB from the aqueous solution. The structural characterization of synthesised polymers has been characterized by standard spectrum analysis. MB adsorption efficiency onto PIEs have been investigated with adsorption parameters such as solution pH, initial MB concentration, adsorbent dosage, contact time and temperature by batch mode studies. Adsorption isotherms, kinetic and thermodynamic parameters of MB onto PIEs have been evaluated using batch adsorption experimental data. The adsorption interaction and its mechanism have been derived based on the spectrum analysis. The reusability of the MB adsorbed adsorbent has been investigated to reduce the hazardous solid waste.

Materials and Methods

Reagents

4,4′-Oxydianiline (ODA), Pyromellitic dianhydrides (PDA) were purchased from Aldrich-Sigma, India, and purified by sublimation and recrystalisation processes. Toluene, N-Methyl-2-pyrrolidone (NMP) and methanol solvents were procured from Thermo Fisher Scientific, India, and purified by distillation method. MB (CI 52015) was supplied by Merck, India. A dye stock solution of 1000 mg/L was prepared using MB. Experimental standard solutions were diluted from the appropriate amount of stock solution using deionized distilled water. Finally, H_2SO_4, KNO_3, HNO_3, HCl and NaOH were procured from Thermo Fisher Scientific, India.

Synthesis of Poly(imide-ether)s

The poly(imide-ether)s (PIEs) adsorbent was synthesized via a two-step process, and the polymerization reaction is shown in the Scheme 2. A double-necked round bottom flask

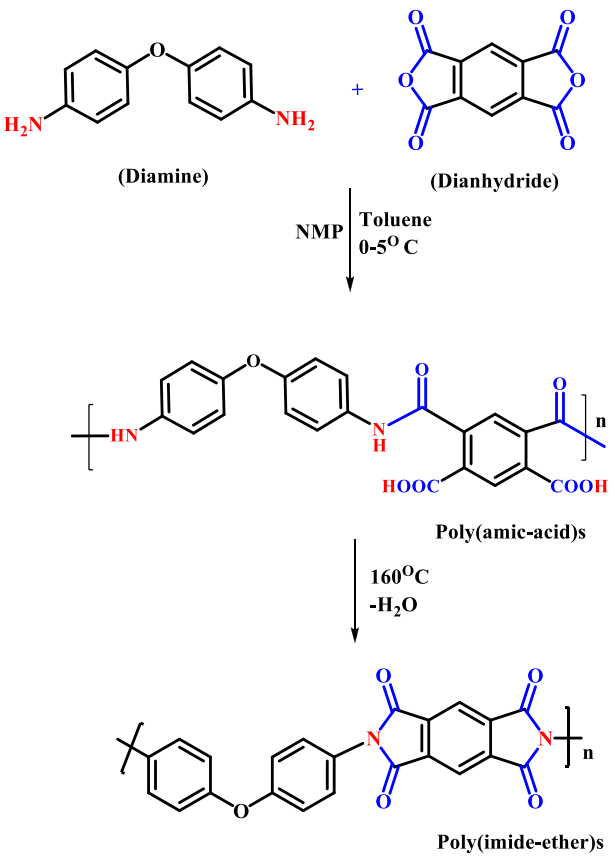

Scheme 2 Synthesis of poly(imide-ether)s

equipped with a Dean-stark distiller and a nitrogen gas inlet and outlet was filled with a homogeneous solid mixture composed of ODA (1 g, 4.994 mmol) dissolved in 20 mL of NMP. Further, (1.089 g, 4.994 mmol) pyromellitic anhydride was added to the reaction flask by adding 40 mL of toluene. The reaction mixture was heated in an oil bath at 160 °C under a stream of nitrogen gas for 6 h, and byproduct (water) was removed during the polymerization. After 1 h, the glass reaction flask was cooled. The solution was filtered, and the filtrate was precipitated by dropwise addition into methanol solvent. The resulting polymer was filtered and dried in a vacuum at 80 °C for 24 h.

Characterization of the Adsorbent and Adsorbed Materials

The structural properties of PIEs were characterized by ^{1}H-NMR (Bruker 400 mhz) and FT-IR (Perkin Elmer, L1860116) and thermal properties were measured by TGA (Perkin Elmer, TGA 4000). The surface properties of PIEs were confirmed by Scanning Electron Microscopy (SEM), Energy Dispersive X-ray spectrometry (EDX) (Quanta 200 FEG) and X-Ray Diffraction (XRD) (Bruker AXS Kappa APEX II CCD). SEM and EDX are very useful to determine the surface morphology and elemental composition of the adsorbent and adsorbed material from a few nanometer depths of the material surface via the electron Back Scattered Detection (BSD) system attached with a microscope. XRD provides the crystalline or amorphous nature of material. All the SEM and EDX analyses of the PIEs and dye adsorbed PIEs were recorded using the Quanta 200 FEG scanning electron microscope at different accelerating voltages with various working distances. The MB concentration in the solutions was measured by using UV–Vis (Perkin Elmer, LAMBDA 1050) spectrophotometer.

Adsorption Studies

Various adsorption parameters such as solution pH, adsorption dosage, contact time and initial dye concentration were optimized to obtain the maximum adsorption capacity. The adsorption experiments were repeated thrice to check the replication and 0–5% of error was observed by the replication process. The adsorption percentage removal was calculated using the Eq. 1.

$$\% \text{ Removal} = \left(\frac{C_0 - C_e}{C_0}\right) \times 100 \quad (1)$$

where, C_o and C_e are the initial and equilibrium concentrations (mg/L) of the dye solutions respectively.

Zero point of Charge (pH_{ZPC}) of PIs

Zero point of charge (ZPC) of PIEs was determined according to standard procedure. 45 mL of 0.1 M KNO_3 solution was taken in a series of 100 mL conical flask. A range of initial pH values of the metal solutions was adjusted at 2, 4, 6, 7, 8, 10 and 12 by using either 0.1 N of HNO_3 or NaOH. 100 mg of the PIEs was added to each flask, and the suspensions were intermittently shaken manually and allowed to equilibrate for 48 h. The MB adsorbed PIEs was removed by the filtration and the final pH of the solution was measured [45].

Reuse of MB Adsorbed–Adsorbent

After adsorption process, adsorbed polymeric material is also one of harmful solid waste, which creates the pollution in the terrestrial ecosystem of the environment. To avoid this problem, the solid waste can be reused to make a useful product without the leaching of adsorbate (metal ions or dye) from the product material. To reduce the solid adsorbent waste, MB adsorbed–adsorbent (PIEs-MB) was used for the preparation of polymer composite with commercial polymer by solution casting method. 50 mg of PIEs-MB polymer composite was immersed into the 50 mL of distilled water and solution kept in a mechanical stirred at 180 rpm for 24 h (temperature maintained 28 °C). PIEs-MB polymer composite was removed and MB leaching properties were examined using the UV–Vis Spectrophotometer.

Results and Discussion

Characterization of the PIEs

The structure of the PIEs was confirmed by the analysis of FT-IR and NMR analysis. The FT-IR spectra of MB, PIEs and PIEs-MB are shown in Fig. 1a–c respectively. The assignment peaks are listed in Table 1. The FT-IR assignments of the peaks of MB are: 1594 (C=N + $(CH_3)_2$ Stretching vibration), 1490 (heterocycle C=S band of middle intensity), 1421 (asymmetric and symmetric vibration of C–H), 1390 (symmetrical and asymmetrical bending vibrations of the CH_3 functional groups of MB), 1334 (Stretching vibrations of the C–N terminal saturated di methyl amino groups), and the lower region becomes difficult to find out the functional group of MB due to rotational structure vibration of C=N and C=C. The FT-IR assignments of PIEs are: FT-IR (ATR) 3122–3638 (end group –NH_2), 1775 (–C=O, sym), 1716 (–C=O, asym), 1601 (Conjugated Phenyl ring), 1501 (–C=C–Ar), 1245 (–C–O–Ar sym), 1065 (–C–O–Ar asym) and 794 (Substituted aryl group) cm^{-1}. The adsorption of MB onto PIEs

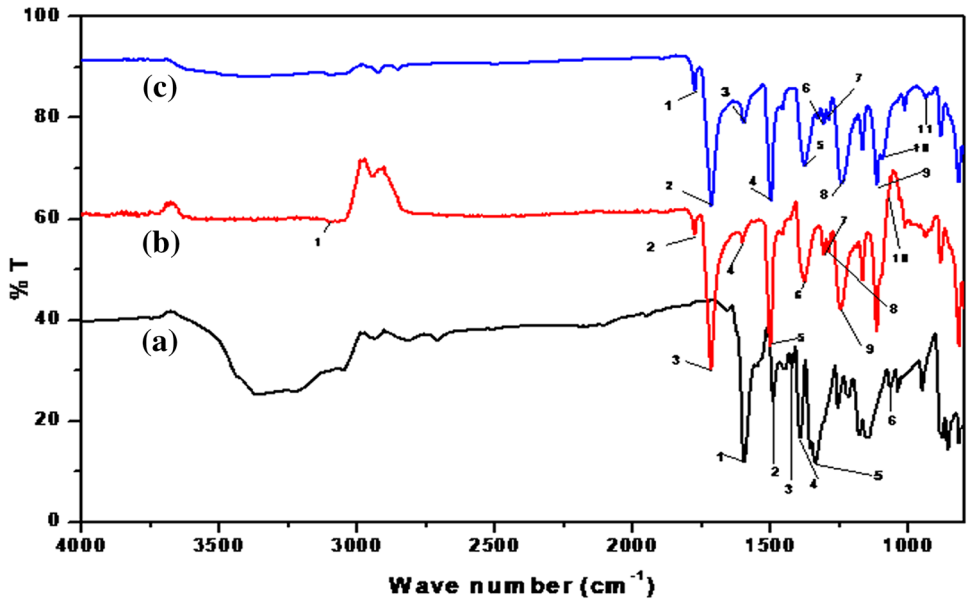

Fig. 1 FT-IR spectra of (a) MB, (b) PIEs and (c) PIEs-MB

Table 1 FT-IR peak assignments of MB, PIEs and MB adsorbed PIEs

FT-IR Wave number cm^{-1}		Peak assignments
MB-(a)		
1	1594	–C=N+$(CH_3)_2$ Stretching vibration
2	1490	Heterocycle C=S band of middle intensity
3	1421	Asymmetric and symmetric vibration of C–H
4	1390	Symmetrical and asymmetrical bending vibrations of the CH_3 functional groups of MB
5	1066	Asymmetric C–S–C vibration
PIEs-(b)		
1	3122–3638	End group –NH_2
2	1775	–C=O, sym stretching
3	1716	–C=O, asym stretching
4	1601	Conjugated Phenyl ring
5	1501	–C=C–Ar stretching
6	1245	–C–O–Ar sym stretching
7	1065	–C–O–Ar asym stretching
8	794	Substituted aryl group
PIEs-MB (c)		
1	1776	–C=O, Sym stretching
2	1714	–C=O, asym stretching
3	1597	–C=N+$(CH_3)_2$ Stretching vibration
4	1498	Heterocycle C=S band of middle intensity
5	1376	(–CO)–O vibration
6	1305	(–CO)–O vibration
7	1240	C=O Vibration
8	1288	Weak stretching vibration of aromatic ether group

(PIEs-MB) attributing the following peaks 1776 (–C=O, Sym), 1714 (–C=O, asym), 1597 –C=N+ $(CH_3)_2$ Stretching vibration, 1498-(heterocycle C=S band of middle intensity) 1376, 1305 (–CO)–O vibration, 1240 (C=O), 1288 weak stretching vibration of aromatic ether group of imide adsorbent.

From the PIEs-MB (Fig. 1c), the cationic auxo chrome group C=N^+ $(CH_3)_2$ and the heterocycle –C=S band of MB

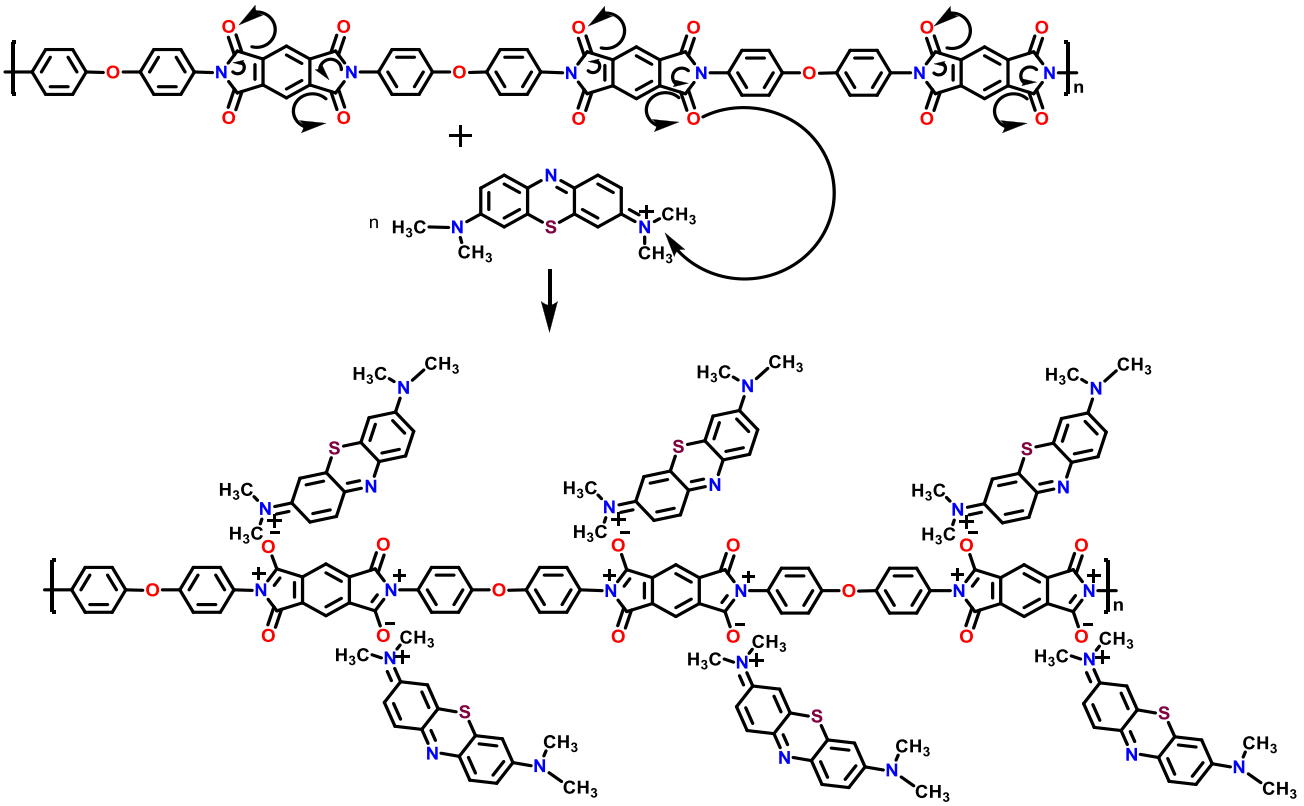

Scheme 3 Intermolecular interaction between MB and PIEs

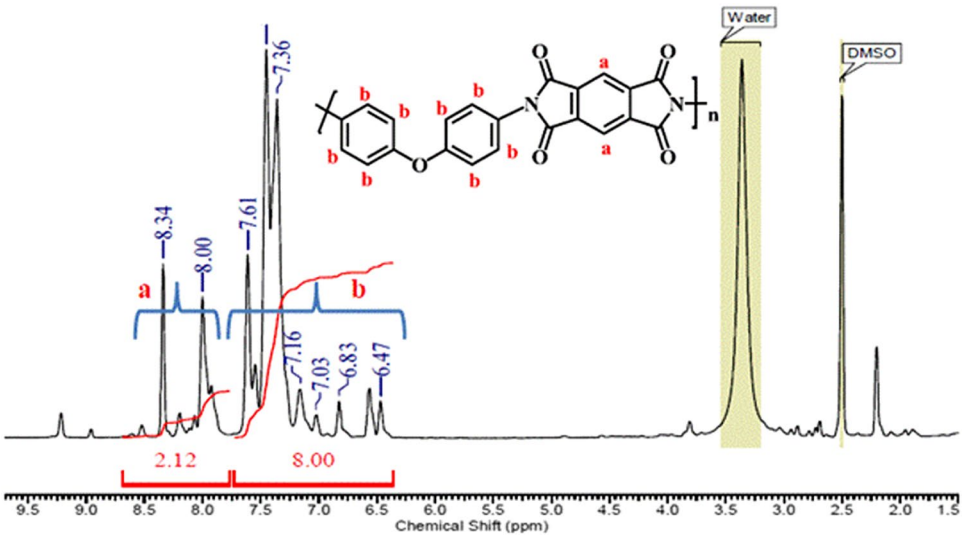

Fig. 2 The ^{1}H-NMR spectrum of PIEs

was observed in the region 1595 and 1490 cm^{-1} respectively. The FT-IR result could suggest that the specific intermolecular interactions occur between the polymer and dye. The carbonyl group of the polyimides acts as binding sites because imide N atom has a lone pair of electron, which could donate the e^{-} to the –C=O group in the imide moieties, and the oxygen becomes more negatively charged. Then the oxygen gains more electron from the nitrogen which behaves as a Lewis base (–N=C–O^{-}) that enhances the activity at the bonding sites. Furthermore, the nitrogen atom of an auxo chrome group (–$N^{+}(CH_3)_2$) in the MB has positive charge that behaves as a Lewis acid (cationic in nature) in the aqueous solution. In such cases Lewis base acts as an electron donor and Lewis acid acts as an electron acceptor, creating

a strong electrostatic attraction (Lewis acid-base) between the N^+ and O^- by intermolecular force and forms the polyimide-dye complex, which is shown in Scheme 3. The FT-IR results could confirm that the MB adsorption occurs on the surface of the PIEs.

The ^{1}H-NMR spectrum of PIEs is shown in Fig. 2. The ^{1}H-NMR assignments of the peaks of PIEs are: ^{1}H-NMR (DMSO-d_6) $\delta = 8.34–8.0$ ppm (2H, diimide substituted phenyl ring) and $\delta = 7.61–6.47$ ppm (8H, diphenylether ring). The signals at $\delta = 2.25$ and 3.50 ppm are due to DMSO-d_6 and moisture respectively. The FT-IR and ^{1}H-NMR analyses confirm that the electron donor and acceptor moieties (Fig. 3) have been successfully incorporated in the structure of PIEs. This could be enhanced with the adsorption behaviour and used for the removal of cationic dyes from the aqueous solution.

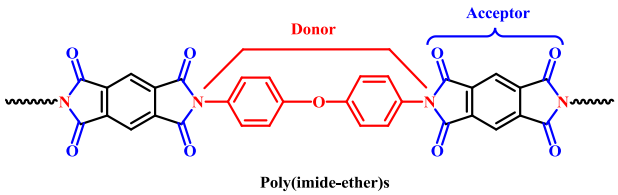

Fig. 3 Electron donor and acceptor segments structure of PIEs

The FE-SEM that was used to validate the change in the morphology of PIEs and MB adsorbed PIEs (PIEs-MB) is represented in Fig. 4. The PIEs SEM image (Fig. 4a) shows a shape of an orchid nodule, a flower which is stacked with a continuous crosslinking chain-like networks. The different particle size of the petals in the flower shaped PIEs SEM image (Fig. 4b) ascribes that the formation of flower shape is due to the inter–intra particulate aggregation. The SEM image of PIEs-MB (Fig. 4c, d) shows the inhabitation of MB molecules on the PIEs, which suggests that the existence of inter-particulate micropores (active binding sites) present abundantly in between the flower aggregation of the PIEs. The results suggest that the adsorbent PIEs, predominantly

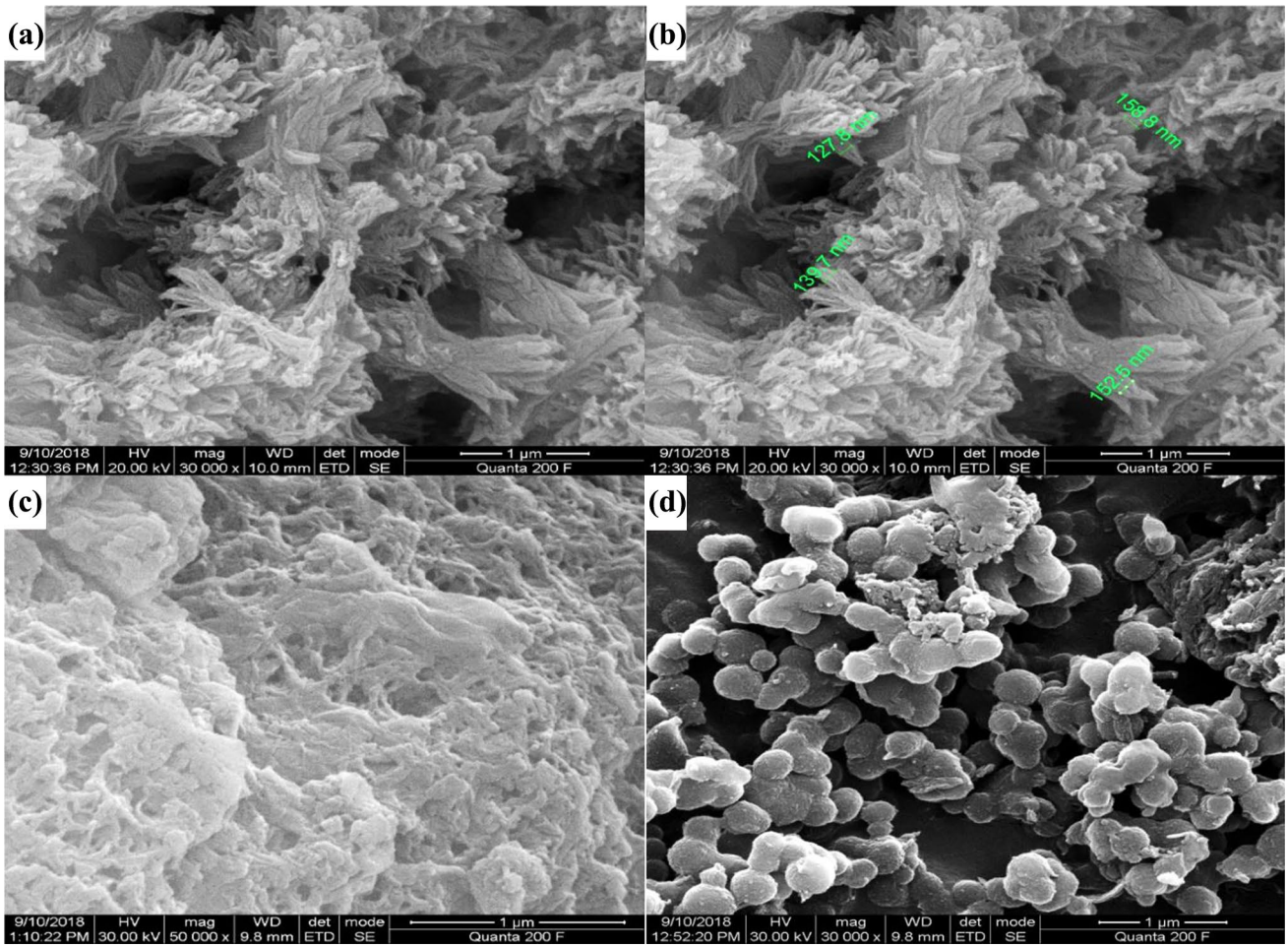

Fig. 4 The SEM images of **a** PIEs, **b** pore size of PIEs, **c** and **d** MB adsorbed PIEs respectively

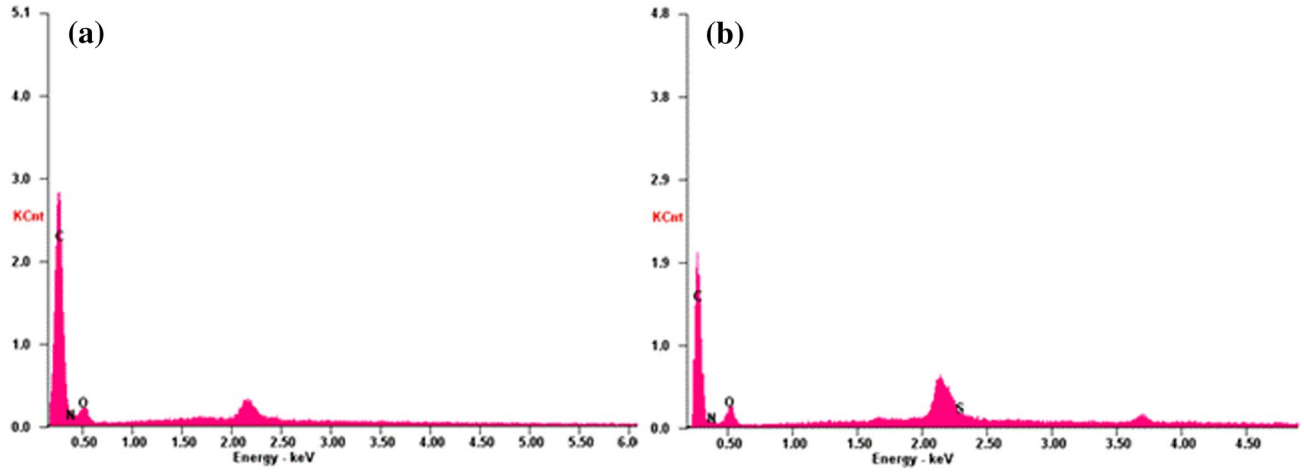

Fig. 5 The EDX spectra of **a** PIEs and **b** MB adsorbed PIEs respectively

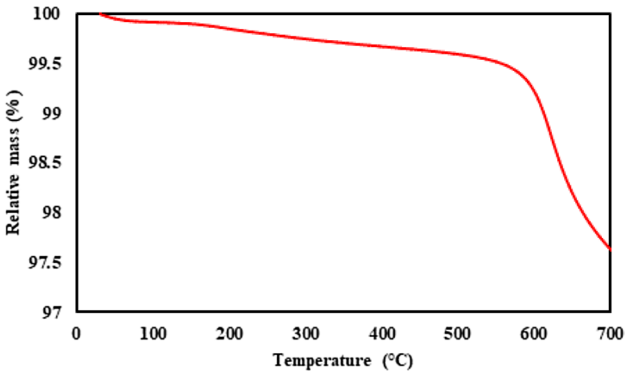

Fig. 6 TG analysis of PIEs

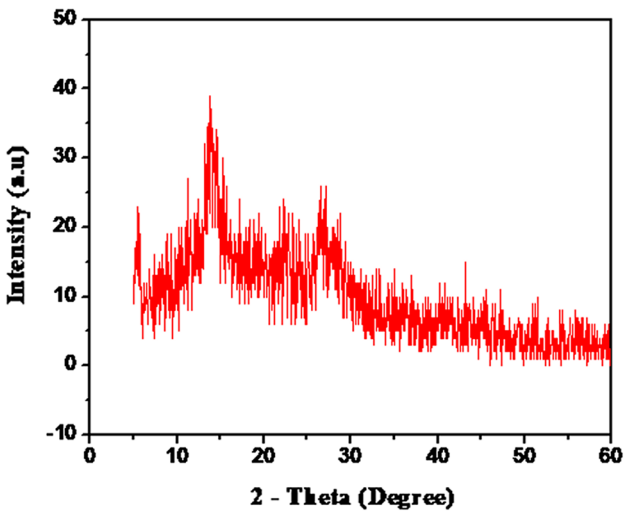

Fig. 7 X-ray diffraction analysis of PIEs

microporous in nature, are the plausible reason for the adsorption of MB dye from aqueous solution.

The EDX spectrum of PIEs and MB adsorbed PIEs (PIEs-MB) are shown in Fig. 5. The process of polycondenzation reaction of a pyromellitic dianhydride (PMDA) and Oxydianline (ODA) to prepare PIEs was noticeable in Fig. 5a with corresponding elemental peaks (C, N, O). Apparently, the removal of MB by PIEs was evident by the spectrum, which is shown in Fig. 5b and the elemental composition of C, N, O, and S further confirms the adsorption is feasible. A peak observed at 2.17 energy intensity (keV) attributes to the gold which is coated on the surface of the polymer material.

The TGA curve of PIEs, shown in Fig. 6, shows that PIEs undergo three stages of degradation. In the first stage, 0.1% of weight loss is observed in the temperature range of 30–120 °C due to the evaporation of the occluded solvent and moisture. Even though the polymers were dried before the thermal analysis, the initial weight loss in the temperature range of 30–120 °C gives evidence of the moisture regaining capacity of the PIEs. At the temperature range 572–642 °C, the second stage of degradation occurs with a weight loss of 0.6–1.7%, which is due the degradation of functional groups in the PIEs. Above 650 °C, a large amount of weight loss was observed, which was due to the decomposition of PIEs. The TG Analysis result suggests that the PIEs is environmentally more stable and adsorption functional moieties or sites could not be affected at ambient temperature.

The XRD analysis of PIEs was performed by using Cu Kα radiation in the range of $2\theta = 5°–60°$ and depicted in Fig. 7. The XRD of PIEs shows a broad diffraction pattern centered at $2\theta \approx 20°$, which reveals that the PIEs is amorphous in nature.

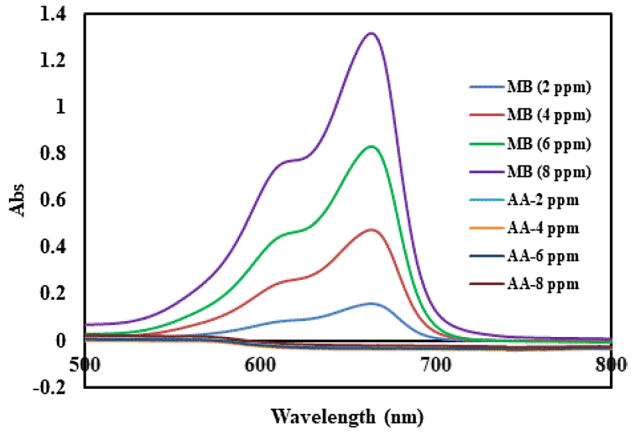

Fig. 8 UV–Vis analysis of MB adsorption onto PIEs

Adsorption Behaviour of PIEs

Synthesized PIEs and stock MB were used as adsorbent and adsorbate respectively in the adsorption process. Initial and final concentrations of MB solutions were determined by UV–Vis analysis. The adsorption parameters were optimized and the data obtained through optimization were evaluated and mechanism of adsorption was predicted with the help of various adsorption (kinetics, isotherms and thermodynamics) models. At first, the adsorption experiment was verified and confirmed with 2, 4, 6 and 8 mg/L of MB concentration solutions and 20 mg of PIEs using UV–Vis analysis, which is shown in the Fig. 8. The MB absorption peaks were observed at the ranges of 608–612 and 658–670 nm, which is in agreement with the theoretical values 609 and 668 nm

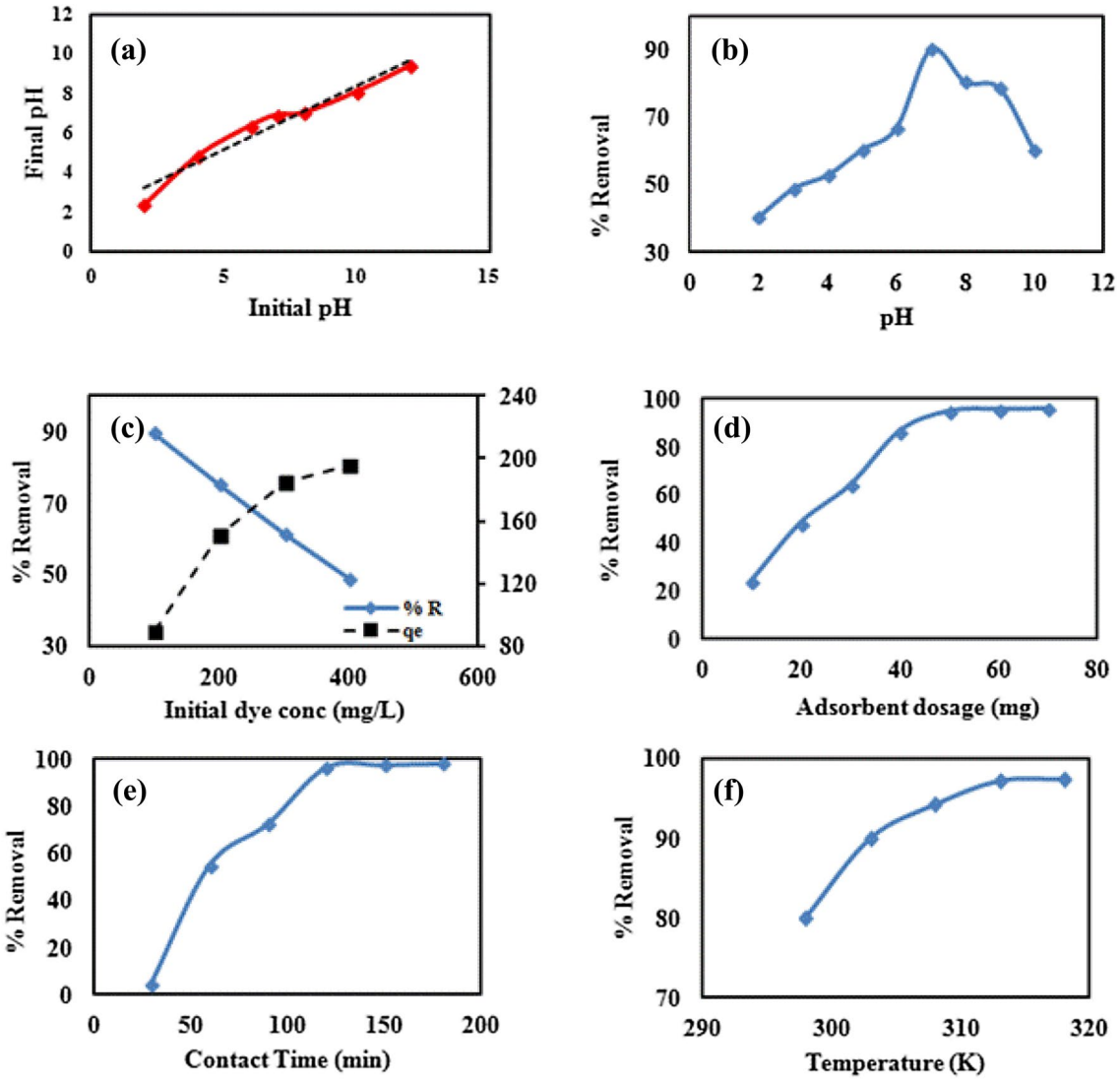

Fig. 9 **a** pH_{ZPC} plot of PIEs and effect of **b** pH **c** initial MB concentration **d** adsorbent dosage **e** contact time and **f** temperature for the adsorption of MB onto PIEs [parameters: pH (2–12), initial MB concentration (100–400 mg/L), adsorbent dosage (10–70 mg), contact time (10–180 min) and temperature (298–318 K)]

respectively. After adsorption process, the MB absorption peaks completely disappeared, which confirms that the adsorption occurred on the surface of PIEs.

Zero Point Charge (pH_{ZPC}) of PIEs

Zero point charge (ZPC) of PIEs was determined by the electrolyte's pH study. pH_{ZPC} curve was plotted by initial pH versus final pH and the result is shown in Fig. 9. From Fig. 9a, the surface electrical charge of PIEs was determined. At pH < pHzpc (below 6.95), the solution pH was increased because the acidic pH solution donates more protons which could be occupied by the adsorbent sites and at pH > pHzpc, the solution pH was decreased due to a reduction of hydroxyl ion by the adsorbent functional moiety in the solution. This result is proposed that the surface charge of the PIEs is negative and positive in nature at lower and higher solution pH respectively. ZPC study also suggests that the PIEs possess the electron donor–acceptor which influence or enhance the adsorption process. The electrical neutral charge (pH_{ZPC}) of PIEs is found to be at pH 6.95, which was maintained in the adsorption experiment.

Effect of Solution pH on the Adsorption of MB onto PIEs

The solution pH is one of the adsorption parameters, and its effect on PIEs was examined using 50 mL of MB solution (200 mg/L of dye concentration) in the pH range 2–10 with an adsorbent dosage of 50 mg of PIEs. The experiment was performed in a mechanical shaker at 180 rpm for 120 min at 28 °C. After adsorption, the MB adsorbed–adsorbent was removed by filtration, and filtrated concentration was measured using the UV–Vis Spectrophotometer.

The effect of solution pH on MB adsorption onto PIEs is shown in Fig. 9b. The hydrogen ions (H^+ in the acidic medium) and hydroxide ions (OH^- in the basic medium) are influenced by the effect of pH study. A lower percentage removal of MB is observed in the acidic medium (At pH 2) because the PIEs surface charge is more negative at lower pH, which may create a strong electrostatic attraction between the negatively charged PIEs and positively charged H^+ ion species. The strong electrostatic attraction cannot be replaced by MB cations, which may be forbidden by the MB cationic adsorption, resulting in lower uptake of MB on the PIEs surface. With an increase in solution pH, the concentration of H^+ ions is reduced, which recreates the binding sites on the PIEs adsorbent. Due to this the percentage adsorption of MB gradually increased up to neutral pH 7. At high pH (after pH 7), the surface charge of PIEs is positive in nature. In the situation, electrostatic repulsion is enhanced between the positively charged PIEs and MB cations, which ultimately reduced the adsorption rate on the surface of PIEs. The maximum adsorption was observed (90%) at neutral pH (approximately 6.95). Hence, the optimum pH value 6.95 was fixed in all the batch adsorption experiments.

Effect of Initial Dye Concentration on the Adsorption of MB onto PIEs

The effect of initial dye concentration was examined using 50 mL of various concentrations of MB solution (100–400 mg/L), and 50 mg of PIs at pH of 6.95 for 120 min and temperature maintained at 28 °C. After adsorption process, the filtrate dye concentrations were measured using the UV–Vis Spectrophotometer. The obtained experimental data were used to evaluate the adsorption isotherm studies.

The effect of initial dye concentration on MB adsorption onto PIEs is shown in Fig. 9c. The adsorption capacity (q_e) and percentage removal of MB was calculated which could be dependent on the active sites on the PIEs and MB concentration. At lower MB concentrations, maximum percentage removal and less q_e of MB onto PIEs were observed. The percentage removal decreased from 89 to 48% and q_e increased from 89 to 195 mg/g with the increase of the MB concentration. At higher MB concentrations, the percentage of MB removal decreased due to the constant and saturation of adsorption sites on adsorbent. After the equilibrium or saturation, more MB was found away from the surface of PIEs in the solution. So, the percentage removal is decreased. Increase in q_e could suggest that the monolayer adsorption occurs on the surface due to the adsorbent–adsorbate interaction (interaction between the functional moieties of PIEs and MB) and followed by multilayer adsorption due adsorbate–adsorbate interaction. It could be concluded that the physisorption and chemisorption takes place on the surface of the PIEs, and it could be further confirmed by evaluation of adsorption isotherm models.

Effect of Adsorbent Dose on the Adsorption of MB onto PIEs

The effect of adsorbent dosage was studied with different adsorbent dosages ranging from 10 to 70 mg of PIEs. These studies were carried out with a 50 mL of MB solution (200 mg/L of dye concentration) in a mechanical shaker at 180 rpm for 120 min. The solution was maintained at 6.95 pH and 28 °C. The final MB concentration was measured using the UV–Vis Spectrophotometer.

The adsorbent dosage also influences the adsorption process and the results are shown in Fig. 9d. The percentage removal of MB onto PIEs increases from 24 to 96% for an increase in the adsorbent dose from 10 to 70 mg. This is due to an increase in the availability of binding sites on the PIEs surface with an increase in the adsorbent dosage. The maximum percentage removal was obtained and saturation occurred with an adsorbent dosage of 50 mg. After saturation, no changes in the adsorption capacity were observed

because of the absence of MB in the solution, and the active sites remained vacant for further adsorption with increasing adsorbent dosage. The findings of the study suggest that the maximum adsorption could be attained with 50 mg of PIEs dose.

Effect of Contact Time on the Adsorption of MB onto PIEs

The effect of contact time is one of the most important adsorption parameters, which was used to evaluate the adsorption kinetic parameters. These studies were also carried out at various contact times between 10 and 180 min with 50 mL of MB solution (200 mg/L of dye concentration) at 6.95 pH. In this study, 50 mg of PIs was stirred at 180 rpm and the temperature was maintained at 28 °C. At regular time intervals between 10 and 180 min, the dye concentration was measured using the UV–Vis Spectrophotometer.

The effect of the contact time for the adsorption of MB onto PIEs is shown in Fig. 9e. The percentage of MB adsorption onto PIEs increased as the contact time was increased and the equilibrium was attained at 120 min. Initially, the rate of adsorption is higher due to a large number of adsorption sites being available for the uptake of the MB from the aqueous medium. After equilibrium, all the adsorption sites were occupied and saturated by the adsorbate. Beyond this, no adsorption was noticed. Hence, in the present study, the optimum adsorption occurred at 120 min, it was chosen as the equilibrium time. The experimental data were further evaluated using adsorption kinetic equations.

Effect of Temperature on the Adsorption of MB onto PIEs

The effect of temperature studies was carried out with different temperatures (298, 303, 308, 313 and 318 K) to evaluate the thermodynamic parameters. The experiment was conducted with 50 mL of MB solution (200 mg/L) and 50 mg of PIEs at pH of 6.95 for 120 min. After the adsorption process, the filtrate dye concentrations were measured using the UV–Vis Spectrophotometer.

Temperature is an important parameter for the adsorption of MB onto PIEs which affects the adsorption capacity. The results are shown in Fig. 9f. From Fig. 9f, it could be observed that the percentage removal increased with increasing temperature upto 308 K. No change was observed in the adsorption percentage after 308 K which suggests that the surface adsorption functional moieties are activated by appropriated temperature and have attained equilibrium. The experimental data were used to further define the thermodynamic parameters such as $\Delta G°$, $\Delta S°$ and $\Delta H°$ and to evaluate the thermal behaviour of MB adsorption onto PIEs.

Adsorption Kinetic Studies

The study of adsorption kinetics is one of the important tools to predict what types of adsorption mechanism takes place on the surface of adsorbent in the adsorption system. The effect of contact time experimental data was used for the investigation of different adsorption kinetic models. The adsorption kinetics studies of MB onto PIEs were evaluated using Pseudo-first order, Pseudo-second order, Elovich and Intra-particle diffusion kinetic models [46–48]. The maximum adsorption capacity of MB onto PIEs at equilibrium (q_e) and time (q_t) mg/g were calculated using the Eqs. 2 and 3 respectively.

$$q_e = \left(C_0 - C_e\right) \times \frac{V}{m} \tag{2}$$

$$q_t = \left(C_0 - C_t\right) \times \frac{V}{m} \tag{3}$$

where, C_t is the concentration of dye in the solution at any time t (mg/L), V is the volume of the solution (L); and m is the mass (g) of the adsorbent.

Pseudo-First Order Kinetic Model

The pseudo-first order equation as is given by Lagergren relates the adsorption rate to the dye adsorbed amount at time t is given in the Eq. 4,

$$\frac{dq_t}{dt} = k_1\left(q_e - q_t\right) \tag{4}$$

where, q_e and q_t are the adsorbed amounts of the dye at equilibrium and time (t) respectively, expressed as mg/g, and k_1 is the pseudo-first order kinetic rate constant, expressed as (min^{-1}). The equation integration and rearrangement yield the linear form is given in the Eq. 5.

$$\log(q_e - q_t) = \log q_e - k_1 t/2.303 \tag{5}$$

The adsorption experimental data of the effect of contact time were used to evaluate pseudo first order kinetic parameters using empirical equation and the results are shown in Fig. 10a. The pseudo-first order equilibrium rate constant (k_{ad}), correlation coefficient (R^2) and equilibrium adsorption capacity (q_e) were calculated from the slope and intercept of the plots of ln (q_e–q_t) Vs t and the constants are listed in Table 2. The R^2 value of the pseudo-first-order kinetic model was found to be 0.9258, which indicates that the adsorption system of PIEs-MB is not fitted well with the experimental data and a slight deviation was observed in the straight line. The q_e value of pseudo-second-order kinetic did not match with the experimental q_e value.

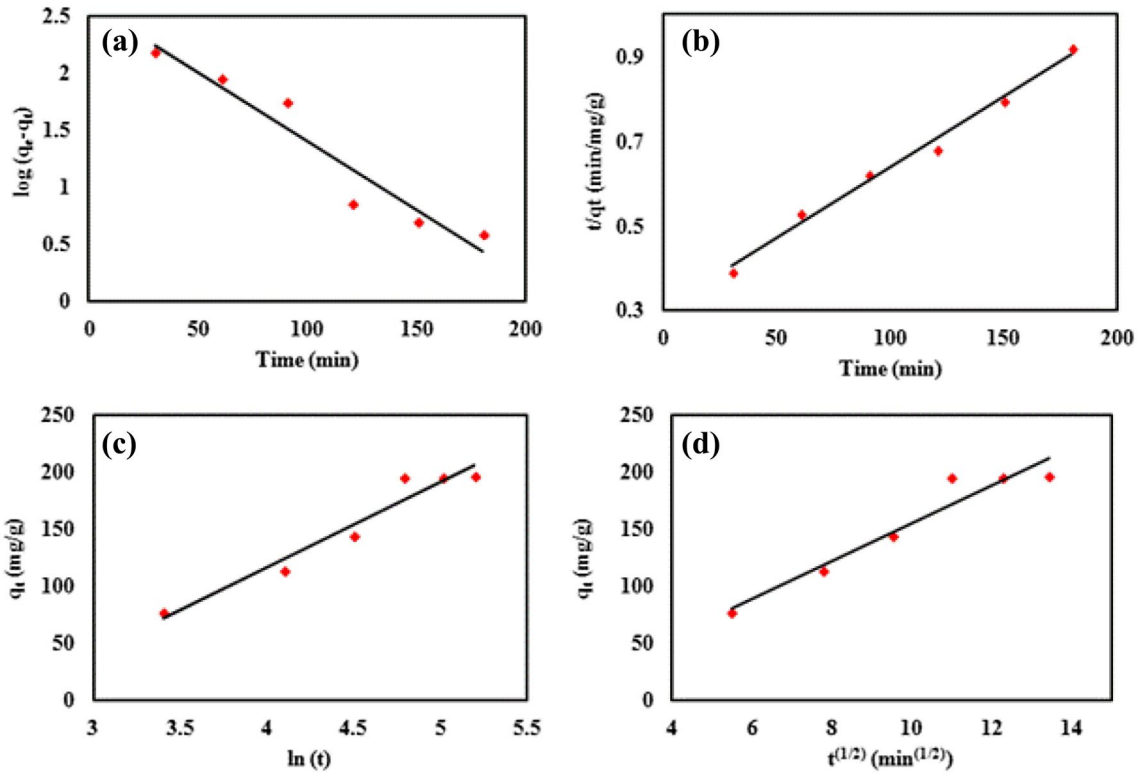

Fig. 10 **a** Pseudo-first order kinetic **b** Pseudo-second order kinetic **c** Elovich model kinetic **d** Intraparticle diffusion model kinetic for adsorption of MB onto PIEs [optimum parameters: pH (6.95), initial MB concentration (200 mg/L), adsorbent dosage (50 mg), contact time (10–180 min) and temperature (303 K)]

Table 2 Kinetic model statistical parameters for adsorption of MB onto PIEs (optimum parameters: pH (6.95), initial MB concentration (200 mg/L), adsorbent dosage (50 mg), contact time (10–180 min) and temperature (303 K)]

Kinetic model	Parameters	MB initial concentration (200 mg/L) MB
Pseudo-first order kinetic model $\ln(q_e - q_t) = \ln q_e - k_{ad}\, t$	k_{ad} (min^{-1})	0.012
	$q_{e,}$ cal (mg/g)	394.9
	R^2	0.9258
Pseudo-second order kinetic model $\frac{t}{q_t} = \frac{1}{k_2 q_e^2} + \frac{1}{q_e} t$	k_2 (g/mg min)	$2.4266 \times 10-5$
	q_e, cal (mg/g)	203
	q_e, exp (mg/g)	198
	R^2	0.9834
Elovich kinetic model $q_t = \frac{1}{\beta} \ln(\alpha\beta) + \frac{1}{\beta} \ln(t)$	α (mg/g min)	11.72
	β (g/mg)	0.0134
	R^2	0.9460
Intraparticle diffusion kinetic model $q_t = k_p t^{1/2} + C$	k_p (mg/g $min^{1/2}$)	15.823
	C	7.0232
	R^2	0.9330

Pseudo-Second Order Kinetic Model

Ho's pseudo-second order kinetic equation is represented in the Eq. 6,

$$\frac{dq_t}{dt} = k_2 (q_e - q_t)^2 \tag{6}$$

where, k_2 (g/mg/min) is the second order kinetic rate constant; the differential equation is usually integrated and transformed in its linear form and given in the Eq. 7.

$$\frac{t}{q_t} = \frac{1}{k_2 q^2} + \frac{t}{q_e} \tag{7}$$

The pseudo-second-order kinetic study was evaluated with the experimental data of the effect of contact time. The parameters (k_2, R^2 and q_e) were derived from the plot of t/q_t against t. The results are shown in Fig. 10b. The value of $q_{e,}$ k_2 and R^2 are listed in Table 2. The obtained R^2 (0.9834) from the straight line defined that the adsorption process of the PIEs- MB system well fitted with the experimental results. Moreover, the obtained q_e value of pseudo-second-order kinetic was relatively close to the experimental q_e value. The R^2 and q_e value of pseudo-second order kinetic

agrees well with the experimental results, which suggests that the adsorption process is dependent on the surface of the adsorbent (PIEs) and the adsorbate (MB).

Elovich Kinetic Model

The experimental data were applied to the Elovich kinetic model, which is given in the Eq. 8,

$$q_t = \frac{1}{\beta}\ln(\alpha\beta) + \frac{1}{\beta}\ln(t) \tag{8}$$

where, α is the initial adsorption rate constant [mg/(g/min)], and the parameter β is related to the extent of the surface coverage activation energy for chemisorptions (g/mg).

The Elovich kinetic equation was used to evaluate the experimental data of the effect of contact time on the adsorption of MB onto PIEs. The values of q_t and ln(t) were calculated and the results are shown in Fig. 10c. The values of α, β and the correlation coefficient (R^2) were calculated from the slope and the intercept of the plot, and the values are listed in Table 2. In the Elovich kinetic plot, the obtained R^2 (0.9460) deviated slightly from pseudo-first and pseudo-second order kinetics. The initial adsorption rate (α) found to be 11.72, could suggests that the MB adsorption onto PIEs is a chemisorption process. The surface coverage activation energy (β) was also found to be 0.0134 g/mg. The derived parameters α and β results could confirm that the adsorption process is more favourable chemisorption followed by physisorption process.

Intraparticle Diffusion Kinetic Model

Weber and Morris derived an equation to express the intraparticle diffusion model and given in the Eq. 9.

$$q_t = k_p t^{1/2} + C \tag{9}$$

where, k_p is the intra-particle diffusion rate constant (mg/g min), and t is the time (min).

The Intraparticle diffusion kinetic equation was also applied to the effect of contact time on the adsorption of MB onto PIEs, and the results are shown in Fig. 10d. The intraparticle diffusion kinetic parameters (k_p, R^2 and C) were derived from the plots of q_t versus $t^{1/2}$ and are listed in Table 2. The double-linear straight line was observed from the plots of q_t versus $t^{1/2}$ and also, this line did not pass through the origin. It seems that the adsorption of MB onto PIEs is feasible, and three stages occur in the adsorption system. In the first stage, the external surface adsorption was attained, and in the second stage, intraparticle diffusion was observed. Finally, the adsorption equilibrium was obtained after the second stage.

From the adsorption kinetic study, the observed result of calculated q_e value of pseudo-first-order kinetic deviated from the experimental q_e value. The R^2 value was found to be 0.9258, which shows that this kinetic model does not fit well with the experimental results. In the pseudo-second-order kinetic model, the obtained q_e value was closer to the experimental q_e values. The R^2 value suggests that the experimental data could be well fitted with pseudo-second-order kinetic model. The rate of initial chemisorption and the surface coverage of adsorbent were defined by the Elovich kinetic parameter of α and β values respectively. The three-stage adsorption diffusion mechanism was derived using the Intraparticle diffusion model. The maximum adsorption capacity (q_e) was found to be 203 mg/g by pseudo-second-order kinetic model, and this model well fits to the experimental data which suggest that the adsorption process of PIEs-MB system follows the second-order kinetic model. Types of adsorption process and the adsorption mechanism were predicted using all four kinetic models. Based on the observed kinetic results, it could be suggested that the PIEs are promising adsorbents for the removal of cationic dye from industrial wastewater.

Adsorption Isotherm Studies

The study of adsorption isotherm is the most important key to identify the type of adsorption process on the surface of adsorbent in the adsorption process. The effect of initial MB concentration date was used to evaluate the non-linear forms of the adsorption isotherm studies. Langmuir, Freundlich, Redlich–Peterson and Sips isotherm parameters were derived with empirical equations using MATLAB R2009a [49].

Langmuir Isotherm Model

The Langmuir isotherm model is very useful tool to determine the characteristics of homogeneous surface and monolayer interaction between adsorbent and adsorbate molecules. The interaction between the adsorbed molecules is negligible. The non-linear equation of the Langmuir isotherm model is expressed in the Eq. 10.

$$q_e = \frac{q_m K_L C_e}{1 + K_L C_e} \tag{10}$$

where, C_e is the equilibrium concentration of the MB in the solution (mg/L), q_e is the adsorbed value of the MB at an equilibrium concentration (mg/g), q_m is the maximum adsorption capacity (mg/g) and K_L is the Langmuir binding constant, which is related to the energy of adsorption.

The Langmuir isotherm dimensionless constant of the separation factor (R_L) values can be used to predict

behaviour of the adsorbent in the adsorption process which is derived using the Eq. 11.

$$R_L = \frac{1}{1 + bC_0} \tag{11}$$

where, b is the Langmuir adsorption equilibrium constant, and C_o is the initial MB concentration.

The Langmuir isotherm model is used to describe the formation of monolayer on the uniform surface of the adsorbent, where the adsorption happens in homogenous active sites. The q_e and C_e experimental data obtained from the study of the effect of initial concentration were fitted with the Langmuir adsorption isotherm equation. R^2 (0.9566), K_L (0.121) and q_m (166.8 mg/g) values were calculated from the plot C_e against q_e by taking intercept, shown in Fig. 11

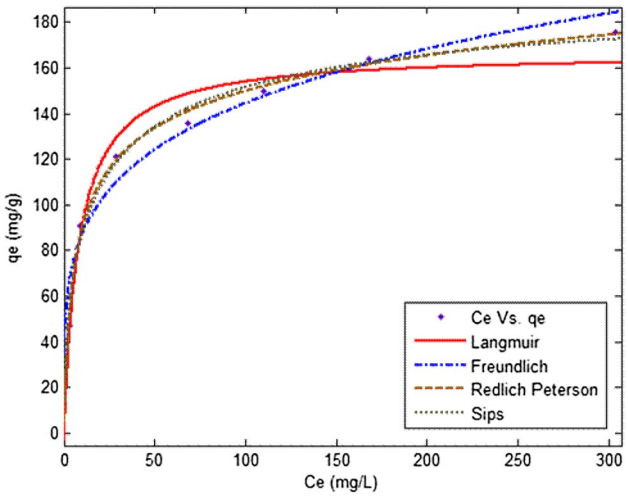

Fig. 11 Non-linear adsorption isotherm for MB adsorption onto PIEs [optimum parameters: pH (6.95), initial MB concentration (100–400 mg/L), adsorbent dosage (50 mg), contact time (120 min) and temperature (303 K)]

which showed that the curve well fitted with the experimental data. All the parameters of the experimental data are listed in Table 3. The R_L values ($0 < R_L < 1$) indicate that the adsorption process is irreversible and support favourable adsorption on PIEs. The R_L (0.02–0.08) and R^2 value suggests the adsorption process of PIEs is monolayer and is a favorable one. The data further suggest the PIEs are better adsorbents for the adsorption of MB.

Freundlich Isotherm Model

The Freundlich isotherm is an important model to predict characteristics of the heterogeneous surface and multilayer adsorption onto the adsorbent. Sorption energy and interaction between the adsorbed molecules also evaluated using this isotherm model. The empirical isotherm equation can be employed to describe the heterogeneity of the adsorption systems and is expressed in the Eq. 12.

$$q_e = K_F C_e^{1/n_f} \tag{12}$$

where, K_F is the Freundlich constant [(mg/g) $(L/mg)^{1/2}$] indicates the adsorption capacity and represents the strength of the adsorption bond, and n_f is the heterogeneity factor which represents the bond distribution. The values of n_f between 1 and 10 indicate favorable adsorption.

The Freundlich isotherm model is not restricted to the monolayer. This is applicable to multilayer adsorption and defines the active site distribution of the adsorbent and surface heterogeneity. The curve was plotted from the adsorption experimental data (q_e and C_e) of the effect of initial concentration using the Freundlich isotherm equation. The isotherm experimental data well fitted with the isotherm expression. The R^2, K_f and n were derived from the plot which is shown in Fig. 11. The value of n_f ˃1shows that the adsorption of PIEs is favorable. All the parameters of the Freundlich isotherm models are listed in Table 3. The R^2

Table 3 Isotherm model statistical parameters for MB adsorption of PIEs [optimum parameters: pH (6.95), initial MB concentration (100–400 mg/L), adsorbent dosage (50 mg), contact time (120 min) and temperature (303 K)]

Isotherm models	Parameters	MB	Isotherm models	Parameters	MB
Langmuir	q_m	166.8	Redlich–Peterson	α	0.3891
	K_L	0.121		β	0.8856
	R_L	0.02–0.08		K_R	35.94
	R^2	0.9566		R^2	0.9923
	SSE	525.7		SSE	93.76
	RMSE	10.25		RMSE	4.841
Freundlich	K_F	52.86	Sips	K_S	0.1943
	n	4.575		n	1.77
	R^2	0.9477		q_m	203.5
	SSE	633.6		R^2	0.9845
	RMSE	11.26		SSE	187.6
				RMSE	6.849

(0.9477) and n_f (4.575) indicate the Freundlich equation is well fitted with the experimental equilibrium data and show the surface heterogeneity of PIEs. The obtained adsorption isotherm results suggest that the multi-layer adsorption occurs on the surface of PIEs.

Redlich–Peterson Isotherm Model

The Redlich–Peterson isotherm is a useful model to predict the homogeneity and heterogeneity of the adsorption system which means a combination of the Langmuir and Freundlich models. It approaches the Freundlich model at higher concentration, and is in accordance with the Langmuir equation at lower concentration. The empirical expression is given in the Eq. 13.

$$q_e = \frac{K_R C_e}{1 + \alpha_R C_e{}^{\beta}} \tag{13}$$

where, K_R is the Redlich–Peterson isotherm constant (L/g), α_R is the Redlich–Peterson isotherm constant (L/mg), and β is the exponent which lies between 0 and 1.

The Redlich–Peterson equation derived from the combination of Langmuir and Freundlich constants suggests that the homogenous and heterogeneous nature of the adsorbent, and it is useful for evaluating the equilibrium data for various concentrations. A plot of C_e against q_e in Fig. 11 is used to determine the Redlich–Peterson parameters (α, K, β) using empirical equation. All the parameters and constants are listed in Table 3. If $(1 - \beta) = 1/n_f$, the adsorption process approaches to the multilayer adsorption of Freundlich isotherm at higher concentration. If $\beta = 1$, the adsorption process approaches to the monolayer adsorption of the Langmuir model at lower concentration. In this model, then β (0.8856) value is nearer to 1, and this confirms that the monolayer adsorption occurred on the surface. The 1- β (0.1144) value is closed to 1/n (0.2815) of Freundlich isotherm model; this confirms the multilayer adsorption is observed on the surface of adsorbent. Based on the analysis of isotherm parameters, large amount of monolayer adsorption and less amount of multilayer adsorption of MB occurred on the surface of PIEs due to its surface heterogeneity, which was confirmed by q_m values of Langmuir (166.8 mg/g) and Sips (36.7 mg/g) isotherm models. The obtained R^2 (0.9923) value confirms, the Redlich–Peterson model is well fitted with the experimental data and follows both the Langmuir and Freundlich isotherm models.

Sips Isotherm Model

The Sips isotherm equation is also the combination of the Langmuir and Freundlich isotherm models. The Sips isotherm model is commonly used to determine the limiting behavior of the adsorbate concentration. The Sips isotherm model equation can be expressed by Eq. 14.

$$q_e = \frac{q_m \left(K_S C_e\right)^{1/n_s}}{1 + \left(K_S C_e\right)^{1/n_s}} \tag{14}$$

where, K_S is the Sips isotherm constant, q_m is the maximum amount of the adsorbed dye per unit weight of the adsorbent (mg/g), and $(1/n_s)$ is the Sips isotherm exponent. The Sips isotherm model is a fusion of Langmuir–Freundlich adsorption model which is applied to determine the restrictive performance of the adsorbate concentration. This model predicts the surface heterogeneity of the adsorption process. According to the adsorbate concentration, this model reduced to Freundlich (multilayer adsorption) isotherm model at lower concentration, but it predicts the Langmuir (monolayer adsorption) isotherm at higher concentration. A plot of C_e against q_e was drawn from the experimental data of effect of initial concentration and shown in Fig. 11. Sips isotherm parameters (K_S, q_m, n_s) were obtained and represented in Table 3. The Sips isotherm exponent $(1/n_s)$ values are found to be 0.4351, which is between 0 and 1. The result of Sips exponent showed that the Langmuir isotherm is more favorable in the adsorption of MB on the surface of PIEs from an aqueous solution, rather than the Freundlich isotherm, which was also confirmed by both the isotherm constants and parameters. The mono and multilayer adsorption capacity (q_m) was observed to 203.5 mg/g and the R^2 (0.9845) value suggests that Sips isotherm is well fitted with the adsorption experimental data. Sips isotherm parameter results also confirmed that the adsorption of MB onto PIEs is a favorable process with heterogeneous surface.

All adsorption isotherm models fitted well with experimental data, which was confirmed by the correlation coefficient (R^2). The monolayer (166.8 mg/g) and multilayer (36.7 mg/g) maximum adsorption capacity ($q_{m)}$ were determined from Langmuir and Sips isotherm model respectively, which suggests that the PIEs is a better adsorbent for the removal of MB from aqueous solution. The adsorption efficiency of MB onto PIEs is very high when compared to earlier literature (Table 4).

Adsorption Thermodynamic Studies of PAC

The thermodynamic parameters (ΔG°, ΔS° and ΔH°) of the adsorption process were evaluated using the experimental data of the effect of temperature [56–58]. This study is very important to solve the practical significant problems in the adsorption process. The change in free energy (ΔG°) of the adsorption system can be estimated with the equilibrium constant using the Eq. 15.

$$\Delta G^{\circ} = -RT \ln K_c \tag{15}$$

Table 4 Comparison of reported adsorbents and its MB adsorption capacity

Adsorbent	Adsorption capacity (mg/g)	References
Coconut coir	15.59	[50]
Wood apple rind	40.1	[15]
Rice husk ash	18.149	[21]
Magnetite/silica/pectin Nano composite	185.18[a] and 197.18[b]	[25]
Magnetite/pectin NC	92.59[a] and 168.72[b]	[25]
Polyaniline zirconium (IV) silicophosphate (PANI-ZSP) nanocomposite	12.0	[51]
Porous poly-melamine-formaldehyde (PMF)	82.5	[52]
Polyaniline filter paper (PANI (EB)-FP)	1.26	[53]
Montmorillonite (MMT)	74	[54]
Polyvinyl alcohol (PVA)	123.3	[55]
PIEs	166.8[a] and 203.5[b]	Present study

[a]Monolayer adsorption

[b]Mono and Multilayer adsorption

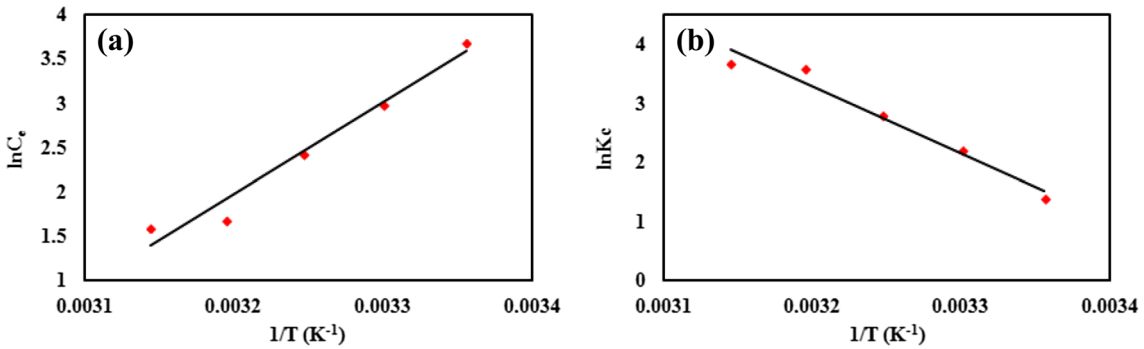

Fig. 12 **a** Plot of $\ln C_e$ against 1/T **b** Plot of $\ln K_c$ against 1/T for MB adsorption onto PIEs [optimum parameters: pH (6.95), initial MB concentration (200 mg/L), adsorbent dosage (50 mg), contact time (120 min) and temperature (298–318 K)]

where K_c is the equilibrium constant (L/g), R is the universal gas constant (8.314 kJ/mol K) and T is the absolute temperature (K). K_c can be determined using the Eq. 16.

$$K_c = \frac{C_a}{C_e} \tag{16}$$

where C_a is the equilibrium dye concentration removed from the solution which assumed as adsorbed on the adsorbent (mg/L), C_e is the equilibrium dye concentration (mg/L).

A straight line is obtained from the plots of ln K_c versus 1/T and the change in enthalpy (ΔH°) and the change in entropy (ΔS°) were observed from the slopes and intercepts of the straight line of plot respectively. ΔH° and ΔS° were derived from the Eqs. 17 and 18.

$$\Delta G^\circ = \Delta H^\circ - T\Delta S^\circ \tag{17}$$

$$\ln K_c = \frac{\Delta S^\circ}{R} - \frac{\Delta H^\circ}{RT} \tag{18}$$

Table 5 Thermodynamic parameters for the adsorption of MB onto PIEs [optimum parameters: pH (6.95), initial MB concentration (200 mg/L), adsorbent dosage (50 mg), contact time (120 min) and temperature (298–318 K)]

Parameters	Temperature (°C)	MB
R^2		0.966
ΔH°(kJmol)		93.734
ΔS° (J/mol)		0.327
− ΔG° (kJ/mol)	298	3.714
	303	5.349
	308	6.984
	313	8.619
	318	10.254

The adsorption thermodynamic study of MB onto PIEs was examined with the effect of temperature data. The thermodynamic parameters, such as Gibbs' free energy change (ΔG°), enthalpy change (ΔH°) and entropy change (ΔS°)

were derived using thermodynamic equations (Eqs. 11–14). ΔH° and ΔS° were defined from the slope and the intercept of the plot of $\ln C_e$ versus 1/T and $\ln K_c$ versus 1/T (Fig. 12a, b). The obtained thermodynamic parameters are listed in Table 5. From the thermodynamic study, the positive enthalpy changes were observed, which reveals that the adsorption process is an endothermic in nature. The negative ΔG° values were observed, which indicate that the adsorption of MB onto PIEs is feasible and spontaneous. The ΔG° value decreased and adsorption capacity increased when temperature increases. From the result of ΔG°, it seems that the PIEs adsorption sites are more active when temperature increases due to decreasing activation energy on the surface of PIEs, which made a fast adsorption interaction between MB and PIEs, So, this adsorption process is more favourable at slightly higher temperature (35 °C). The results of thermodynamic studies suggest that the PIEs could be a promising adsorbent for the removal of cationic dye from the aqueous solution and is more favourable at higher temperatures.

Conclusion

In this study, anionic chelating (imide and ether groups) PIEs was successfully synthesized and used for the removal of cationic MB dye from the aqueous solution. The anionic chelating functional groups enhanced the adsorption efficiency and it could be dependent upon the adsorption parameters such as solution pH, adsorbent dosage, contact time and initial MB concentration. It was optimized. The adsorption kinetic results showed that the q_e value derived from the pseudo second order kinetic was very close with experimental q_e value and obtained experimental data well fitted with pseudo second order kinetic. It could be suggested that the adsorption of MB onto PIEs followed the pseudo second order kinetics. Two (Langmuir and Freundlich) and three (Redlich–Peterson and Sips isotherms) parameter isotherm was derived with the effect of initial MB concentration experimental results. It could be suggested that the PIEs has heterogeneous surface. The monolayer (adsorption capactiy 166.8 mg/g) and multilayer (adsorption capactiy (32.7 mg/g) adsorption efficiency were observed from Lanmuir and Sips parameters respectively. The negative ΔG° and positive ΔH° and ΔS° values of adsorption thermodynamic study indicate that the nature of adsorption of MB onto PIEs is an endothermic reaction and the process is feasible and spontaneous. High adsorption efficiency was observed when compared to earlier reports and adsorbed waste material could be converted into a useful polymer composite to avoid solid waste in the environment. Based on the adsorption experimental results, we suggested that the PIEs could be a considerable potential adsorbent for the removal of cationic dyes from the aqueous solution due to its adsorption efficiency and reusability.

Acknowledgements AM thanks the SSN Trust and Institutions for the grant of the Internal Funded Faculty Project. PR, NNAB and KJT thanks the SSN Trust and Institutions for the award of Internally Funded Student Project (Grant No. IFFP-CHEM-2017).

References

1. Zhu L, Chen L, Wu X, Ding X (2018) Ecol Indic 91:470–477
2. Feng D, Bai B, Wang H, Suo Y (2018) J Polym Environ 26:567–588
3. Agnihotri S, Singhal RJ, Polym Environ (2018) 26:383–395
4. Novais RM, Ascensao G, Tobaldi DM, Seabra MP, Labrincha JA (2018) J Clean Prod 171:783–794
5. Novais RM, Carvalheiras J, Tobaldi DM, Seabra MP, Labrincha JA (2019) J Clean Prod 207:350–362
6. Dalvand A, Khoobi M, Nabizadeh R, Ganjali MR, Gholibegloo E, Mahvi AH (2018) J Polym Environ 26:3470–3483
7. Shourijeh ZM, Montazerghaem L, Olya ME (2018) J Polym Environ 26:3550–3563
8. Murugesan A, Vidhyadevi T, Kirupha SD, Ravikumar L, Sivanesan S (2012) Environ Prog Sustain Energy 32:673–680
9. Vidhyadevi T, Murugesan A, Kalaivani SS, Anilkumar M, Thiruvenkada Ravi KV, Ravikumar L, Anuradha CD, Sivanesan S (2014) Environ Prog Sustain Energy 33:855–865
10. Sun L, Chen D, Wan S, Yu Z (2018) J Polym Environ 26:765–777
11. Zawani Z, Luqman CA, Choong TSY (2009) Eur J Sci Res 37:67–76
12. Mohammadi M, Hassani AJ, Mohamed AR, Najafpour GD (2010) J Chem Eng Data 55:5777–5785
13. Gong R, Ye J, Dai W, Yan X, Hu J, Hu X, Li S, Huang H (2013) Ind Eng Chem Res 52:14297–14303
14. Kavitha D, Namasivayam C (2007) Bioresour Technol 98:14–21
15. Malarvizhi R, Ho YS (2010) Desalination 264:97–101
16. Malik PK (2004) J Hazard Mater 113:81–88
17. El Nemr A, Abdelwahab O, El-Sikaily A, Khaled A (2009) J Hazard Mater 161:102–110
18. Preethi S, Sivasamy A, Sivanesan S, Ramamurthi V, Swaminathan G (2006) Ind Eng Chem Res 45:7627–7632
19. Robinson T, Chandran B, Nigam P (2002) Water Res 36:2824–2830
20. Senthilkumar S, Kalaamani P, Porkodi K, Varadarajan PR, Subburaam CV (2006) Bioresour Technol 97:1618–1625
21. Chowdhury AK, Sarkar AD, Bandyopadhyay A (2009) Clean-Soil Air Water 37:581–591
22. Wang S, Zhu ZH (2006) J Hazard Mater 136:946–952
23. Wang S, Li H, Xu L (2006) J Colloid Interface Sci 295:71–78
24. Karadag D, Akgul E, Tok S, Erturk F, Kay MA, Turan M (2007) J Chem Eng Data 52:2436–2441
25. Attallah OA, Al-Ghobashy MA, Nebsen A, Salem MY (2016) RSC Adv 6:11461–11480
26. Banerjee S, Gautam RK, Jaiswal A, Chattopadhyaya MC, Sharma YC (2015) RSC Adv 5:14425–14440
27. Das SK, Khan MM, Parandhaman T, Laffir F, Guha AK, Sekaran G, Mandal AB (2013) Nanoscale 5:5549–5560
28. Naeem H, Ajmal M, Muntha S, Ambreen J, Siddiq M (2018) RSC Adv 8:3599–3610
29. Nassar MY, Khatab M (2016) RSC Adv 6:79688–79705
30. Nassar MY, Ali EI, Zakaria ES (2017) RSC Adv 7:8034–8050
31. Sun L, Hu S, Sun H, Guo H, Zhu H, Liu M, Sun H (2015) RSC Adv 5:11837–11844

32. Xiao J, Lv W, Xie Z, Tan Y, Song Y, Zheng Q (2016) J Mater Chem A 4:12126–12135
33. Guzman KAD, Taylor MR, Banfield JF (2006) Environ Sci Technol 40:1401–1407
34. Murugesan A, Vidhyadevi T, Kalaivani SS, Premkumar MP, Ravikumar L, Sivanesan S (2012) Chem Eng J 197:368–378
35. Mobinikhaledi A, Moghanian H, Safari P, Firuzian E (2018) J Inorg Organomet Poly Mater 28(3):631–642
36. Murugesan A, Ravikumar L, Sathya Selva Bala V, SenthilKumar P, Vidhyadevi T, Dinesh kirupha S, Kalaivani SS, Krithiga S, Sivanesan S (2011) Desalination 271:199–208
37. Mobaraki Z, Moghanian H, Faghihi K, Shabanian M (2018) J Inorg Organomet Poly Mater 28(3):1072–1089
38. Aref L, Navarchian AH, Dadkhah D (2018) J Polym Environ 25:628–639
39. Faghihi K, Moghanian H, Mozafari F, Shabanian M (2018) Chin J Poly Sci 36(7):822–834
40. Ozbas Z, Demir S, Kasgoz H (2018) J Polym Environ 26:2096–2106
41. Shao H, Chen N, Li S, Lin F, Jiang J, Ma X (2017) Polym 9(12):734–744
42. Ravikumar L, Kalaivani S, Vidhyadevi T, Murugasen A, Kirupha SD, Sivanesan S (2014) Open J Polym Chem 4:1–11
43. Kumar M, Vijayakumar G, Tamilarasan R (2018) J Polym Environ. https://doi.org/10.1007/s10924-018-1318-0
44. Dafader NC, Rahman N, Majumdar SK, Khan MMR, Rahman MM (2018) J Polym Environ 26:740–748
45. Hasan SH, Ranjan D, Talat M (2010) Bio Resour 5(2):563–575
46. Lagergren S (1898) K Sven Vetensk akad Handl 24:1–39
47. Ho YS, McKay G (1999) Process Biochem 34:451–465
48. Weber WJ, Morris JC (1963) J Sanit Eng Div 89:31–60
49. Ayawei N, Ebelegi AN, Wankasi D (2017) J Chem 5:1–11
50. Sharma YC, Upadhyay SN (2009) Energy Fuels 23:2983–2988
51. Gupta VK, Pathania D, Kothiyal NC, Sharma G (2014) J Mol Liq 190:139–145
52. Wang Y, Xie Y, Zhang Y, Tang S, Guo C, Wu J, Lau R (2016) Chem Eng Res Des 114:258–267
53. Majumdar S, Saikia U, Mahanta D (2015) J Chem Eng Data 60:3382–3391
54. Zhou K, Zhang Q, Wang B, Liu J, Wen P, Gui Z, Hu Y (2014) J Clean Prod 81:281–289
55. Agarwal S, Sadegh H, Monajjemi M, Hamdy AS, Ali GAM, Memar AOH, Shahryari-Ghoshekandi R, Tyagi I, Gupta VK (2016) J Mol Liq 218:191–197
56. Khan AA, Singh RP (1987) Coll Surf 24(1):33–42
57. Ramesh A, Lee DJ, Wong JW (2005) J Coll Interface Sci 291:588–592
58. Chiu H, Wang J (2009) J Environ Protect Sci 3:102–106